Hindawi
Science and Technology of Nuclear Installations
Volume 2020, Article ID 5945718, 16 pages
https://doi.org/10.1155/2020/5945718

Research Article

Supercritical CO_2 Brayton Cycle Design for Small Modular Reactor with a Thermodynamic Analysis Solver

Pan Wu,[1] **Chuntian Gao**,[1] **Yanping Huang**,[2] **Dan Zhang**,[3] **and Jianqiang Shan**[1,4]

[1]*School of Nuclear Science and Technology, Xi'an Jiaotong University, No. 28 Xianning West Road, Xi'an, Shaanxi, China*
[2]*CNNC Key Laboratory on Nuclear Reactor Thermal Hydraulics Technology, Nuclear Power Institute of China, Chengdu 610041, China*
[3]*Science and Technology on Reactor System Design Technology Laboratory, Nuclear Power Institute of China, Chengdu 610041, China*
[4]*The State Key Laboratory of Multiphase Flow in Power Engineering, Xi'an Jiaotong University, Xi'an 710049, China*

Correspondence should be addressed to Pan Wu; wupan2015@mail.xjtu.edu.cn and Jianqiang Shan; jqshan@mail.xjtu.edu.cn

Received 13 September 2019; Revised 25 November 2019; Accepted 26 December 2019; Published 24 January 2020

Academic Editor: Arkady Serikov

Coupling supercritical carbon dioxide (S-CO_2) Brayton cycle with Gen-IV reactor concepts could bring advantages of high compactness and efficiency. This study aims to design proper simple and recompression S-CO_2 Brayton cycles working as the indirect cooling system for a mediate-temperature lead fast reactor and quantify the Brayton cycle performance with different heat rejection temperatures (from 32°C to 55°C) to investigate its potential use in different scenarios, like arid desert areas or areas with abundant water supply. High-efficiency S-CO_2 Brayton cycle could offset the power conversion efficiency decrease caused by low core outlet temperature (which is 480°C in this study) and high compressor inlet temperature (which varies from 32°C to 55°C in this study). A thermodynamic analysis solver is developed to provide the analysis tool. The solver includes turbomachinery models for compressor and turbine and heat exchanger models for recuperator and precooler. The optimal design of simple Brayton cycle and recompression Brayton cycle for the lead fast reactor under water-cooled and dry-cooled conditions are carried out with consideration of recuperator temperature difference constraints and cycle efficiency. Optimal cycle efficiencies of 40.48% and 35.9% can be achieved for the recompression Brayton cycle and simple Brayton cycle under water-cooled condition. Optimal cycle efficiencies of 34.36% and 32.6% can be achieved for the recompression Brayton cycle and simple Brayton cycle under dry-cooled condition (compressor inlet temperature equals to 55°C). Increasing the dry cooling flow rate will be helpful to decrease the compressor inlet temperature. Every 5°C decrease in the compressor inlet temperature will bring 1.2% cycle efficiency increase for the recompression Brayton cycle and 0.7% cycle efficiency increase for the simple Brayton cycle. Helpful conclusions and advises are proposed for designing the Brayton cycle for mediate-temperature nuclear applications in this paper.

1. Introduction

The study of supercritical carbon dioxide (S-CO_2) Brayton cycle becomes popular in engineering area because of its merits of high cycle efficiency, configuration compactness, and lower purification system requirements compared with the steam Rankine cycle [1]. Its application area has extended to the industries of nuclear [2], fossil fuel, waster heat, solar energy [3, 4], etc. In the role of power conversion system for nuclear energy, the conceptual studies of S-CO_2 Brayton cycle working as direct cooling system have been widely carried out for the 2400 MW_{th} fast reactor [5], 200 MW_{th} gas fast reactor (SC-GFR) [6], and 36.2 MW_{th} micro modular reactor [7, 8] and also as an indirect cooling system of small modular sodium-cooled fast reactor [9, 10] and lead fast reactor [11]. All these studies are preliminary feasibility analyses of Brayton cycle working with nuclear application, which is summarized in the paper of Pan Wu [12].

A small modular reactor (SMR) can help meet clean energy goals and make electricity more accessible for all. SMR using the S-CO_2 Brayton cycle as its indirect power

cooling system owns the advantage of high cycle efficiency and high system compactness. High compactness indicates that the nuclear power system has the possibility to be transported through trucks or ships, which means construction schedule reduction and lower cost for overall construction. SMR coupling with the S-CO_2 Brayton cycle could be used to bring electricity to remote communities and mining or military bases. Additionally, the S-CO_2 Brayton cycle has a less efficiency decrease when using dry air to discharge the system waste heat, compared with the cases using water as the heat sink. China has a large area which needs electricity and lack of adequate water resources in northwest district. SMR coupling with the S-CO_2 Brayton cycle is a perfect solution to this problem.

In this paper, a naturally circulated 100 MW_{th} lead-cooled small modular reactor (SNCLFR-100) which has a mediate core-outlet-temperature is selected as the target analysis object [13]. Higher core-outlet-temperature is always attractive to researchers because it can bring higher cycle efficiency. However, higher core-outlet-temperature will also bring problems of structural material corrosion, which is still a tricky problem for lead fast reactors. Lowering the core-outlet-temperature is helpful to mitigate this problem, and the application of S-CO_2 Brayton cycle is helpful to offset the cycle efficiency decrease caused by low core-outlet temperature. In this paper, design of the simple and recompression S-CO_2 Brayton cycle is carried out to study if the S-CO_2 Brayton cycle could achieve high thermal efficiency under mediate-core-outlet-temperature, which makes this nuclear system own the characteristics of high compactness and high efficiency. An in-house steady thermodynamic analysis solver named SASCOB is developed to evaluate and optimize the simple and recompression Brayton cycle configuration for the lead fast reactor under different cooling conditions (including water-cooled and dry-cooled conditions). The cycle parameter effects, such as compressor inlet pressure and temperature, turbine inlet pressure, recuperator conductance, and recompression compressor flow ratio, are studied to optimize the best Brayton cycle configuration for the 100 MW_{th} LFR. The model developed in this paper is a powerful tool for conceptual design and thermodynamic analysis of the nuclear reactor system coupled with the S-CO_2 Brayton cycle. The cycle parameter effects on thermal efficiency are helpful for the S-CO_2 Brayton cycle design for nuclear applications.

2. Description of Lead Fast Reactor and Typical S-CO_2 Brayton Cycle Configuration

Corrosion of structural material caused by high-temperature lead makes mediate-outlet-temperature core design easy to be realized. Due to the low hydraulic friction inside the core and the thermodynamic properties of lead, the lead fast reactor (LFR) owns the potential to transport the reactor power totally via effective natural circulation. LFR has great safety performance under steady and transient conditions [13]. At the same time, the coolant of LFR has stable chemical characteristics and does not react with water or air. This feature makes the LFR system possible to eliminate the intermediate cooling circuit, which is needed in the sodium fast reactor system. That is the reason why the lead fast reactor is selected as the power source for the S-CO_2 Brayton cycle.

2.1. Description of Lead Fast Reactor. The heat source of our Brayton cycle design comes from a typical pool-type lead fast reactor SNCLFR-100 [13], which is a 100 MWth lead-cooled small modular reactor with a passive cooling feature under both normal and abnormal operations proposed by University of Science and Technology of China (USTC). SNCLFR-100 incorporates some innovative ideas such as integral arrangement, modular design, and natural coolant circulation, which will help simplify the system design and improve the reactor safety performance and engineering feasibility. The original design parameters of SNCLFR are listed in Table 1.

Another big feature of SNCLFR-100 is its designed core outlet temperature of 480°C. As we all know, higher core outlet temperature means higher turbine inlet temperature, which could help produce very high power conversion efficiency. However, coolant lead at high temperature will bring corrosion problems for the core materials, which is still not solved for LFR development. Thus, a mediate core outlet temperature is benefit for material selection during the core design and improves the engineering feasibility of LFR.

The feature of fully natural coolant circulation increases the inherent safety performance of SNCLFR-100 under both normal and abnormal operation scenarios. Calculation results [13] show that SNCLFR-100 is able to guarantee a sufficient safety margin for fuel melting and other constrains considered under accidents of unprotected transient overpower and unprotected loss of heat sink [14].

2.2. Description of Typical S-CO_2 Brayton Cycle Configuration. The S-CO_2 Brayton cycle applies supercritical carbon dioxide as coolant, instead of steam, to transport thermal energy produced by heat source to the gas turbine, which converts the thermal energy to mechanical energy. So why do we use S-CO_2 as the transport medium? As can be seen in Figure 1, S-CO_2 has a very high density and compressibility near its critical point. Using the compressor driven by the turbine to compress the high-density CO_2 could save the consumed power and increase the cycle efficiency. Evidence shows that the S-CO_2 Brayton cycle has higher cycle efficiency than that of the steam Rankine cycle and other Brayton cycles using gases like He and nitrogen, when the turbine inlet temperature is higher, 550°C (Figure 2).

Figure 3 shows the two typical S-CO_2 Brayton cycle configurations, which are simple Brayton cycle (SBC) and recompression Brayton cycle (RBC), respectively. For SBC which is shown in Figure 3(a), the coolant near CO_2 critical point (7.4 MPa and 31°C) at point 5 is circulated and pressurized by the compressor first. Then, the coolant at point 6 flows through the recuperator and is heated by the hot side flow of the recuperator. The coolant at point 7 absorbs the heat through directly heating or indirectly heating by the heat source and the temperature rise to a high

Table 1: Main design parameters of SNCLFR-100 [13].

Design parameter	Values or characteristics
Reactor thermal power	100 MW_{th}
Refueling interval	10 years
Coolant/heat transport system	Lead/compact pool-type
Reactor inlet temperature	400°C
Reactor outlet temperature	480°C
Cooling mode	Fully natural circulation
Mass flow rate through the core	8528 kg/s
Fuel	MOX
Cladding	T91
Core height	3400 mm
Active zone height	1000 mm
Equivalent core diameter	3460 mm

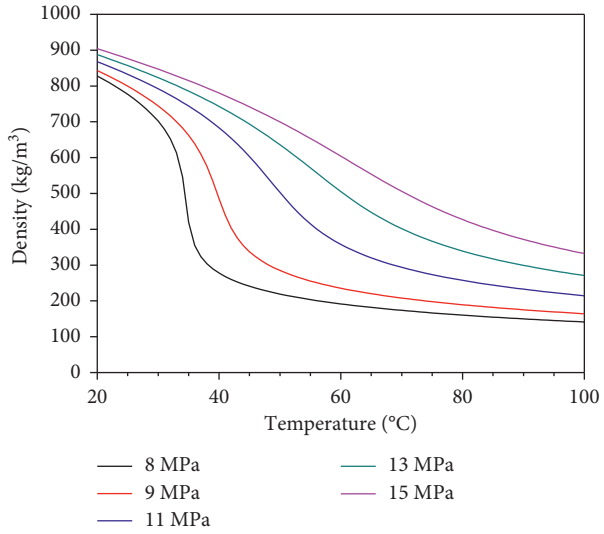

Figure 1: CO_2 density variation with temperature under supercritical pressures.

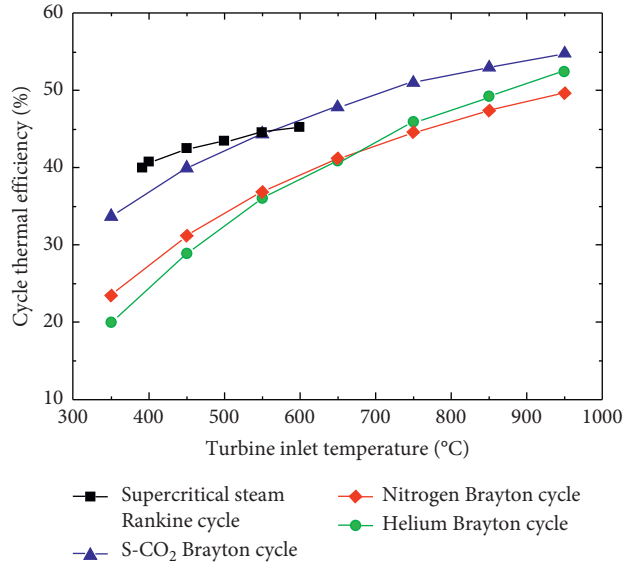

Figure 2: Power cycle efficiency comparison between different power conversion systems.

level. Then coolant of high pressure and high temperature at point 1 enters the gas turbine and drives the shaft to rotate. The compressor, generator, and turbine share the same rotating shaft, which is also a way to improve the cycle efficiency. Coolant leaving the turbine then enters the low-pressure high-temperature side of the recuperator, and the heat is recuperated to heat the cold side flow at high pressure. After leaving the recuperator, the coolant is further cooled by the precooler (heat sink) to be close to the CO_2 critical point. This is the coolant flow path in SBC. However, in SBC, there is only one recuperator and the pinch point in the recuperator restricts the further efficiency improvement of SBC. Based on SBC, MIT proposed the RBC configuration, which adds a recompression compressor and splits the original recuperator into a high-temperature recuperator (HTR) and a low-temperature recuperator (LTR), to solve the pinch point problem [15], (Figure 3(b)). Calculation results show that RBC could effectively increase the cycle efficiency than SBC [15].

Besides the advantage of high efficiency compared with helium Brayton cycle and steam Rankine cycle at the reference temperature considered for this study, the S-CO_2 Brayton cycle has the advantage of high compactness. CO_2 has a higher heat transfer capacity compared with other gases, which can help reduce the size of the heat exchanger. The high-density property of CO_2 makes the CO_2 turbine much smaller than that of helium or steam turbomachinery. Take the turbine size as an example, CO_2, helium, and steam turbine size is about 1 : 6 : 30 under same turbine output power [16]. Additionally, the S-CO_2 Brayton cycle keeps single phase all the time during the operation, which makes the system quickly respond to the load change or system disturbance, and has less risk of flow instability.

There are also other Brayton cycle configurations, for example, intercooling, double recompression or reheating S-CO_2 Brayton cycle [17]. The benefits of these Brayton cycle is still under investigation. However, all of these mentioned Brayton cycles will result in more complex configuration, which complicates the control system. That is the reason why only SBC and RBC are studied in our paper.

3. Code Development and Validation of Integrated Thermodynamic Analysis Code

3.1. Mathematical Modeling for Brayton Cycle. The main physical models of SASCOB include turbomachinery model and heat exchanger model. Gas compressor and turbine are the main turbomachinery model in the S-CO_2 Brayton cycle. The compressor is a machinery which pressurizes low-pressure gas to high-pressure gas through consuming mechanical energy. In this paper, a lumped parameter method will be applied to evaluate the steady state performance of compressor. Parameters of pressure ratio and efficiency are used to describe the compressor thermal performance.

Figure 4 shows the fluid enthalpy and entropy variation during ideal and realistic compression process. The ideal compression process is regarded as an isentropic process, and the realistic compression process need a factor of

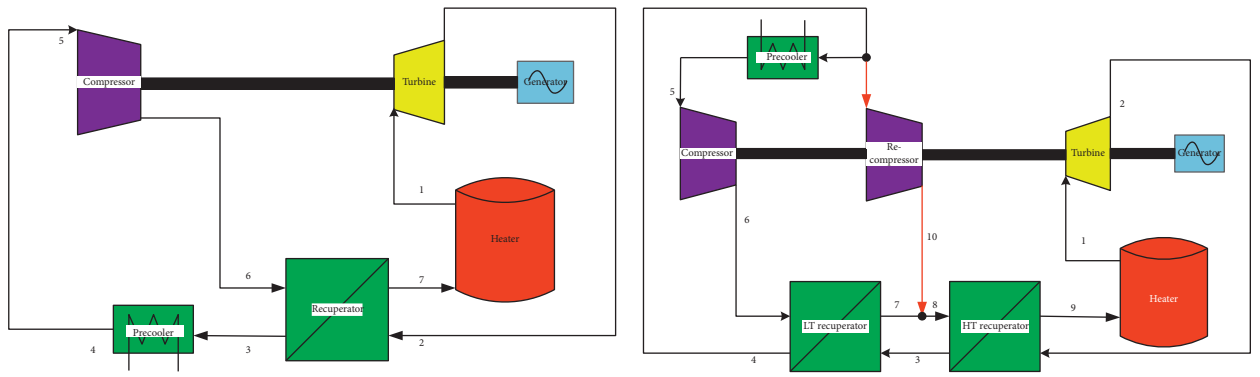

Figure 3: Schematic of typical Brayton cycle used in nuclear application. (a) Simple Brayton cycle; (b) recompression Brayton cycle.

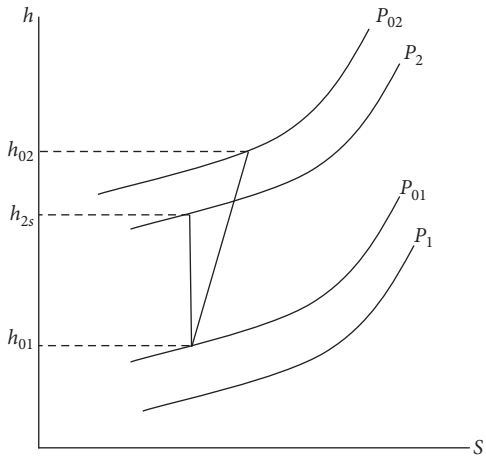

Figure 4: Ideal and realistic compression processes inside the compressor.

compressor adiabatic efficiency to account for the additional enthalpy increase compared with that of the ideal process.

By knowing the pressure ratio r_c and the inlet pressure of compressor P_{c1}, the outlet pressure p_{c2} of the compressor can be calculated by

$$p_{c2} = p_{c1} r_{mc}, \tag{1}$$

With the inlet temperature T_{c1} and pressure P_{c1} and the principle that ideal thermal process through the compressor is an isentropic process, the ideal outlet entropy s_{c2s} and enthalpy h_{c2s} are

$$s_{c2s} = s_{c1}(p_{c1}, T_{c1}), \tag{2}$$

$$h_{c2s} = h(p_{c2}, s_{c2s}). \tag{3}$$

The actual outlet enthalpy h_{c2} can be derived from inlet enthalpy h_{c1}, ideal outlet enthalpy h_{c2s}, and the compressor efficiency η_{mc}:

$$h_{c2} = \frac{h_{c1} + (h_{c2s} - h_{c1})}{\eta_{mc}}. \tag{4}$$

Thus, the temperature of coolant at the outlet of compressor T_{c2} can be obtained by the following equation:

$$T_{c2} = T(p_{c2}, h_{c2}). \tag{5}$$

The power consumed by compressor can be calculated as follows:

$$W_{mc} = \dot{m}(h_{c2} - h_{c1}), \tag{6}$$

With the pressure ratio and efficiency of the compressor, the compressor outlet condition can be derived from the inlet condition through equations (1) to (6).

A turbine is used to convert the thermal energy of coolant to mechanical energy. The lumped parameter method which is similar to that of the compressor model is applied here to solve the turbine model with the aid of parameters of pressure ratio and efficiency.

There are three heat exchangers in the recompression supercritical CO_2 Brayton cycle, which are low-temperature recuperator, high-temperature recuperator, and precooler. As the heat exchanger may be the largest component in the Brayton cycle under such a large heat exchange demand, the compactness of the heat exchanger is very important. The printed circuit heat exchanger developed by HEATRIC Company has the advantage of high compactness, high-pressure bearing capacity, and wide application scope, which satisfy the heat exchange requirement of the S-CO_2 Brayton cycle. Figure 5 shows cross section of the PCHE heat exchanger, whose flow channel is made by semicircle horizontal flow tubes, with hot and cold fluid flow channels alternatively configured.

The conductance is selected to express the heat transfer capacity and size of the heat exchange instead of effectiveness. The concept of effectiveness is not applied due to the fact that it will cause dramatical variation of the conductance value for a given heat load under different design conditions. For example, designing recuperator using the same heat transfer effectiveness results in very large difference in the recuperator heat transfer conductance, which can be easily found in Table 3 of [18].

In order to reduce the calculation error, the heat exchanger is divided into N parts through the channel. The UA value of the total heat exchanger can be obtained through equation (7), which is closely related to the inlet and outlet temperature at hot and cold sides of the recuperator. The UA

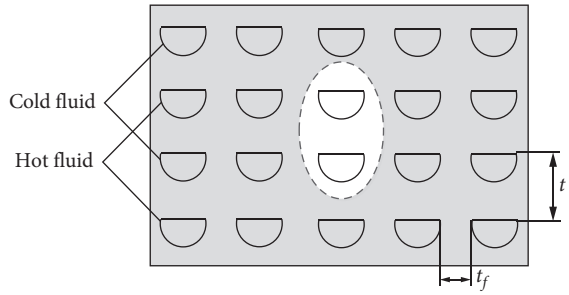

Figure 5: Cross section of the printed circuit heat exchanger.

calculation method refers to Dyreby's paper [19] and the reader could find the detailed methodology of calculating NTU and $C_{\min}$ in Appendix A:

$$\mathrm{UA} = \sum_{i=1}^{N} \left(\mathrm{NTU}_i * C_{\min,i}\right). \tag{7}$$

In the integrated model of SASCOB, the input parameters include inlet temperature, inlet pressure, efficiency and pressure ratio of compressor and turbine, efficiency and pressure ratio of recompression compressor, required UA values of each recuperator, fraction of the flow rate flowing into recompressor, and total heat added to the Brayton cycle. The outlet condition of the compressor and turbine can be obtained by using the turbomachinery model. By knowing the temperature at state points 2 and 6, a random value between value of T2 and T6 can be assigned to T3 and further a random value between value of T3 and T6 can be assigned to T4. By knowing the temperature at state point 3, state point 4, and state point 6, the conductance of the low recuperator can be achieved with equation (7). The value of T4 is adjusted to make the conductance of the low recuperator satisfy the required value set by the user. After the iteration calculation for the low recuperator, the model proceeds to the calculation for the high-temperature recuperator by adjusting the value of T3. When the conductance of the low recuperator and high recuperator both meet the user requirement, the temperature value at point 3, point 4, point 7, and point 9 is confirmed. The mass flow rate of the Brayton cycle will be calculated by

$$\dot{m} = \frac{Q_{\mathrm{heat}}}{h_1 - h_9}. \tag{8}$$

The Brayton cycle efficiency can be achieved through

$$\eta_{\mathrm{brayton}} = \frac{W_t - W_{mc} - W_{rc}}{Q_{\mathrm{heat}}}. \tag{9}$$

The detailed calculation process is found in Appendix B.

In the calculation process, the thermal property of S-CO_2 is calculated by the in-house property package [12]. The in-house property package is made up of polynomial correlation fitted based on CO_2 property data from NIST REFPROP. The thermal property package covers pressure range of 0.1–20 MPa and temperature range of 0–991°C. Parameters including entropy, temperature, specific volume, conductivity, and dynamic viscosity have been obtained through the pressure and enthalpy. The in-house package predicted the CO_2 property very well in most property range with a relative error lower than 0.5%. Detailed information could be found in [12].

3.2. Validation of SASCOB. Pope [20] proposed a 2400 MW_{th} reactor concept which is directly cooled by the S-CO_2 recompression Brayton cycle. The main parameters of its S-CO_2 Brayton cycle are listed in Table 2. Inlet temperature and pressure of the turbine are 650°C and 20 MPa, and the inlet temperature and pressure of the main compressor are 32°C and 7.69 MPa, which make the cycle achieve a high cycle efficiency of 50%.

Using the detailed parameters (power, heat exchanger size, mass flow rate, turbomachinery pressure ratio, and efficiency) described in Pope's paper [20], SASCOB is able to get the overall cycle conditions. Figures 6 and 7 show the comparison of pressure-specific volume map and temperature and entropy map between values calculated by SASCOB and from the MIT designed cycle. From the figure, we can see that the property values at different point calculated by SASCOB is very close to those MIT design values.

The maximum relative error and average relative error for pressure are 0.33% and 0.17%, while the maximum relative error and average relative error for temperature are 0.85% and 0.25%. The results indicate that the developed code SASCOB is able to predict the Brayton cycle parameters with a very small relative error. Table 3 lists the comparison of some important parameters for the recompression Brayton cycle. The loop mass flow rate is 11931 $\mathrm{kg\,s^{-1}}$, the recompression compressor flow ratio is 40.7%, while the cycle efficiency is 49.7%. When compared with the MIT design value, the relative errors of these three key parameters are 1.9%, 3.1%, and 0.6%, which also demonstrates SASCOB's ability in predicting the overall cycle parameters.

4. Brayton Cycle Design for Lead Fast Reactor

As mentioned in the previous section, SNCLFR-100 owns a thermal power of 100 MW and inlet and outlet temperatures of 400°C and 480°C. In this paper, the design of the CO_2/lead intermediate heat exchanger is not included. Olumayegun et al. assume the turbine inlet temperature as 530°C when its core outlet temperature is 545°C [21]. ABR-1000 coupled with S-CO_2 cycle owns an outlet core temperature of 488°C and turbine inlet temperature of 472°C [22]. The lead fast

Table 2: Cycle design parameters of MIT 2400 MW_{th} recompression Brayton cycle.

Main parameters	Value
Inlet pressure of main compressor (MPa)	7.69
Inlet temperature of main compressor (°C)	32
Main compressor efficiency (%)	90.6
Main compressor pressure ratio	2.61
Recompression compressor efficiency (%)	90.0
Turbine efficiency (%)	94.1
Turbine inlet temperature (°C)	650

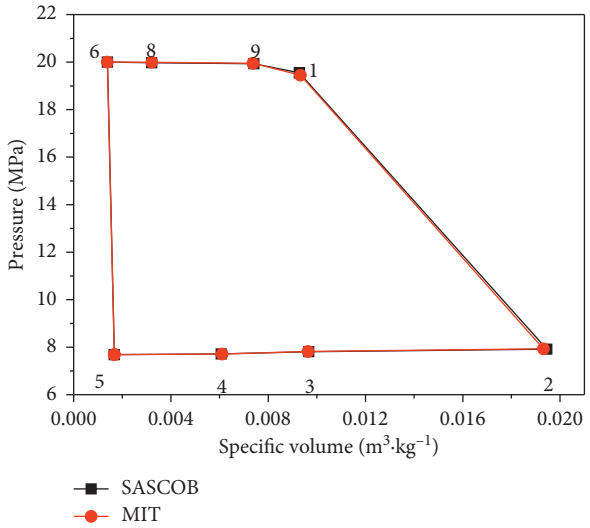

Figure 6: Specific volume comparison between calculated and MIT design values.

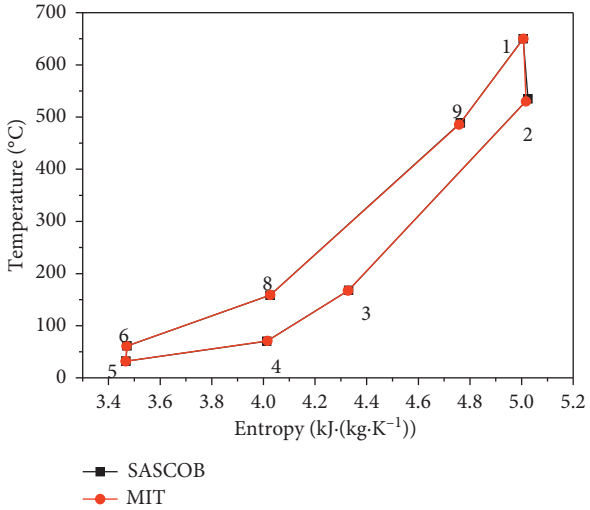

Figure 7: Temperature-entropy comparison between calculated and MIT design values.

reactor system coupled with the S-CO_2 Brayton cycle mentioned in paper of Moisseytsev et al. has a core outlet temperature of 578°C and an inlet turbine temperature of 560°C [23]. In this paper, the outlet temperature of the secondary side of the intermediate heat exchanger is assumed to be 20°C lower than core outlet temperature, which is conservative compared with the design of the abovementioned reference. The detailed design of the intermediate heat exchanger should be done in the future to accomplish this goal. The thermal input for the S-CO_2 Brayton cycle equals to the core thermal power of 100 MW. Under water-cooled condition, the cooling capacity of the secondary system is considered to be efficient and the compressor inlet temperature should be confirmed through sensitivity analyses. Under dry-cooled condition, the coolant capacity of the secondary system is assumed to be weak. Thus, the minimum of compressor inlet temperature varies from 35°C to 55°C, which finally depends on the air dry cooling system design.

The cycle efficiency mainly depends on cycle operation conditions, such as maximum pressure and temperature, minimum pressure and temperature, recuperator conductance, recompression fraction (only for recompression cycle), and turbomachinery efficiency. As the maximum temperature has already been set to 460°C, other cycle parameters should be optimized. The cycle parameters are initially set referred to existing literature [24], as shown in Table 4. The effects of compressor and turbine operation condition is first investigated to get the optimal SBC design under water-cooled condition and dry-cooled condition. After that, the effects of the recompression flow ratio and the heat exchanger conductance are investigated under water-cooled condition and dry-cooled condition.

4.1. Optimal Design for Simple Brayton Cycle

4.1.1. Effects of Compressor Parameters. In order to study the effects of compressor parameters, the heat exchanger conductance and the turbine inlet pressure for SBC included in Table 4 are kept constant. The compressor inlet temperature varies from 30°C to 55°C at different compressor inlet pressures. From Figure 8, we can see that the compressor working close to the critical point or pseudocritical point can achieve the peak cycle efficiency at a certain CIP value. For the working area of CIP around 7.4 to 8.0 MPa, the highest cycle thermal efficiency is reached when the CIP equals to 7.4 MPa and CIT is about 32°C, which is around 34.13%. This phenomenon indicates that the compressor inlet condition should stay closer to the critical or pseudocritical point to get high thermal efficiency. However, the CO_2 properties, like density, specific heat, and conductance, vary sharply around the critical or pseudocritical point, which will bring huge difficulty in controlling the secondary water flow of the precooler. Staying away from the critical point helps eliminate this problem. When CIP equals to 7.4 MPa, 1°C away from the critical or pseudopoint, it brings around 0.3% cycle efficiency reduction. The optimal compressor inlet temperature needs to be determined also by evaluating the controllability of the compressor inlet temperature. On the other hand, the CIP temperature is determined by the precooler condition. When the precooler is set to be cooled by air, CIT at the compressor will increase. When air cooling is considered and the CIT is assumed as 55°C, the cycle

Table 3: Comparison of cycle parameters between SASCOB result and MIT design value.

Parameters	SASCOB	MIT design point	Relative error (%)
Loop mass flow rate (kg·s^{-1})	11,931	11,708	1.9
Recompression compressor flow ratio (%)	40.7	42.0	3.1
Cycle efficiency (%)	49.7	50.0	0.6

Table 4: Initial cycle parameter for simple and recompression Brayton cycles.

Parameter	Simple Brayton cycle	Recompression Brayton cycle
P_{min} (MPa)	7.4	7.4
P_{max} (MPa)	20	20
T_{min} (°C)	32	32
T_{max} (°C)	460	460
UA/MW/K	2	LTR/HTR 2.911/2.089
φ	—	0.3
ε_{com}	0.89	0.89
ε_{recom}	—	0.89
ε_{tur}	0.93	0.93

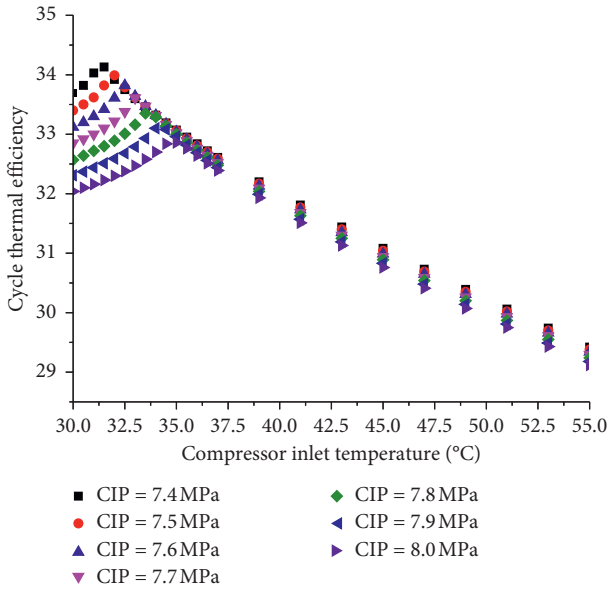

Figure 8: Effects of compressor inlet temperature (CIT) and compressor inlet pressure (CIP) on the cycle thermal efficiency for SBC.

efficiency is 4.7% lower than that of simple Brayton cycle configuration whose CIT is close to the critical point at CIP of 7.4 MPa.

Another interesting phenomenon is that, when the CIT increases to certain value, for example, 35°C, CIP plays a less important role in determining the cycle efficiency. In the working condition area of CIT larger than 35°C, 1 MPa CIP increase brings 0.47% cycle efficiency reduction.

4.1.2. Effects of TIP. As the turbine inlet temperature (TIT) is constrained by the lead fast reactor outlet temperature, which is set as 460°C in this paper, only effects of turbine inlet pressure (TIP) on cycle thermal efficiency are considered in this part. In this section, the parameters for SBC in Table 4 are kept constant excluding TIP. Figure 9 shows the variation of cycle thermal efficiency and turbomachinery work with the turbine inlet pressure change. With higher TIP, the turbine will produce more work and the compressor also consumed more work due to large pressure rise. The balance between turbine produced work and compressor consumed work results in the increase of thermal efficiency with increase of TIP. Higher TIP helps increase the cycle thermal efficiency. However, it is also interesting to see that the efficiency increase rate decreases with further rise in TIP. For the cases where TIP is lower than 20 MPa, TIP increase of 1 MPa brings around thermal efficiency increase of 0.93%. For the cases where TIP is higher than 25 MPa, TIP increase of 1 MPa only brings around thermal efficiency increase of 0.13%. At the same time, higher system pressure raises a stricter requirement on the manufacture of pipe and heat exchangers. For these two considerations, 20 MPa is set as the optimal turbine inlet pressure.

4.1.3. Effects of Heat Exchanger. Increasing the heat exchanger conductance is helpful to recycle more heat through recuperator and reduce the heat discharged into the heat sink, which further increase the cycle thermal efficiency. In this section, the parameters for SBC in Table 4 are all kept constant excluding the heat exchanger conductance. Figure 10 shows the effects of heat exchanger UA on the cycle thermal efficiency for SBC when the values of CIP and CIT, as well as TIP and TIT, are set as 7.4 MPa/32°C and 20 MPa/460°C. From the figure we can see that, when heat exchanger UA rises, the outlet temperature of recuperator's high-pressure side (HP) increases and the outlet temperature of the recuperator's low-pressure side (LP) decreases, which indicate that more power is recovered by the recuperator. As the HP outlet temperature of the recuperator equals to the inlet temperature at the heat exchanger (HX), more cycle mass flow rate is needed to accomplish the set HX outlet temperature of 460°C. High cycle mass flow rate makes the turbine to produce more work and the compressor to consume more power. It is obvious that the rise of turbine produced power is higher than that of the compressor consumed power, which indicates that more net power is produced by SBC and cycle thermal efficiency increases.

However, there is a limit in designing recuperator UA that the minimum temperature difference (min_dt) between hot and cold sides of the recuperator should be over 10°C to avoid the pinch point [25]. When the minimum temperature difference is less than 10°C, very large HX volume is needed to increase the recuperator power by a little bit, which is not economical. The dash line in Figure 10 represents the

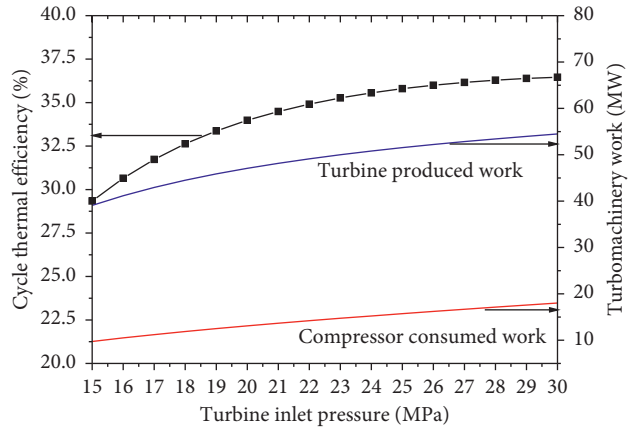

Figure 9: Effects of TIP on the cycle thermal efficiency for SBC.

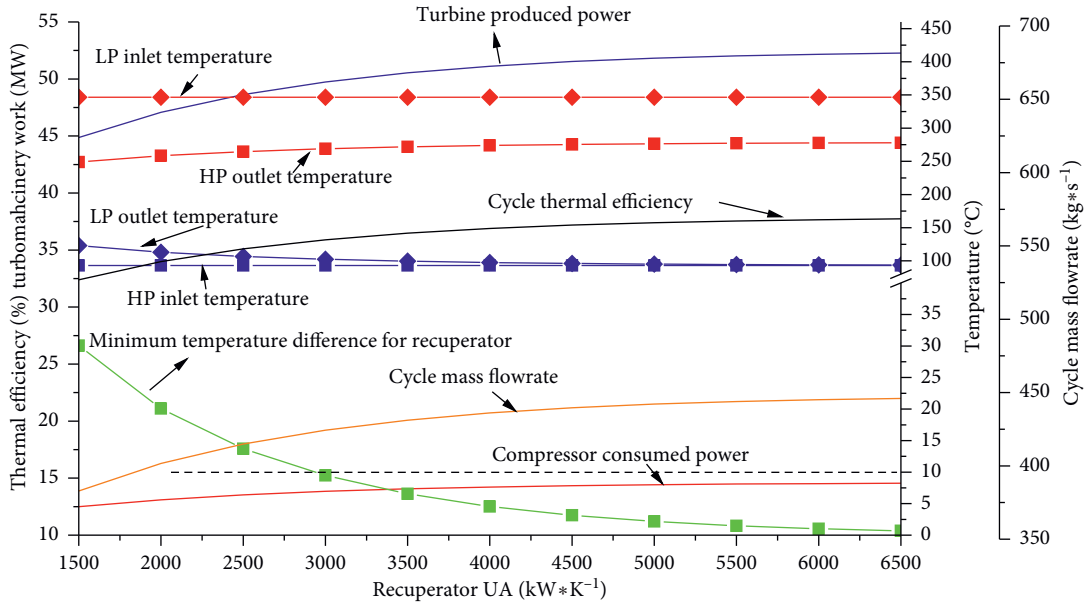

Figure 10: Effects of the heat exchanger UA on the cycle thermal efficiency for water-cooled SBC.

minimum temperature difference of 10°C. It is worth noting that the maximum recuperator conductance of 3 MW/K satisfies the requirement of the recuperator pinch point. Therefore, for SBC, the optimal cycle efficiency of 35.9% is obtained when the recuperator conductance equals to 3 MW/K.

For dry-cooled SBC, the compressor inlet temperature could vary from 40–60°C depending on the weather and air cooling tower design [26]. The calculation result of dry-cooled SBC at various compresses inlet temperatures between 40°C and 60°C is shown in Figure 11. It is clearly shown that, for a given compressor inlet temperature, the cycle efficiency increases with the increase of the recuperator UA. When considering the limit value for recuperator min_dt to be 10°C, there is a maximum cycle efficiency for each case. The maximum cycle efficiencies for conditions whose compressor inlet temperature equals to 40°C, 45°C, 50°C, and 55°C are 34.8%, 34.1%, 33.3%, and 32.6%, respectively. Every 5°C decrease on the compressor inlet temperature will bring around 0.7% efficiency increase for the simple Brayton cycle. However, lower compressor inlet temperature needs the air cooling system to consume more power. The selection of proper compressor inlet temperature for dry-cooled SBC should be made by considering the power consumption of the air cooling system and the overall cycle thermal efficiency. The design and analysis for the air cooling system will not be expanded in this paper.

The detailed cycle configuration of optimized SBC for water-cooled (CIT of 32°C) and dry-cooled conditions (regard CIT value as 55°C) is listed in Table 5.

4.2. Optimal Design for Recompression Brayton Cycle

4.2.1. Effects of Compressor Parameters. In the effect study of compressor parameters, the parameters for RBC excluding compressor inlet temperature and inlet pressure in Table 4

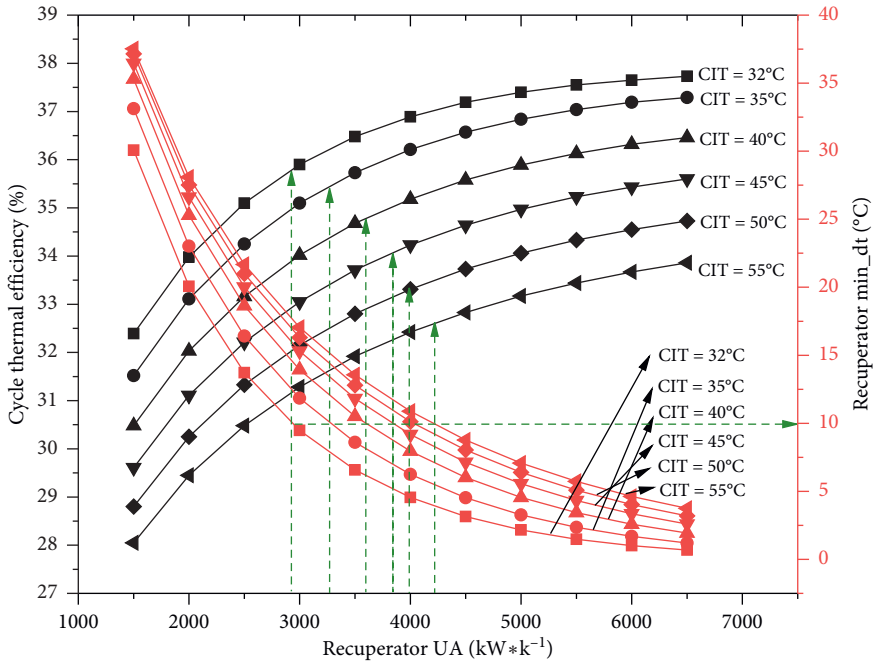

Figure 11: Effects of the recuperator UA on the cycle thermal efficiency for dry-cooled SBC.

Table 5: Optimal design for the water-cooled simple Brayton cycle.

Cooling type	Water cooled	Dry cooled
Produced net power	35.9 MW	32.6 MW
Cycle thermal efficiency	35.9%	32.6%
Turbine mass flow rate	426.3 kg/s	515.0 kg/s
TIP/TIT	20 MPa/460°C	20 MPa/460°C
CIP/CIT	7.4 MPa/32°C	7.4 MPa/55°C
Recuperator UA	3000 kW/K	4200 kW/K
Inlet and outlet temperatures of high-pressure side of recuperator	94.0°C/269.8°C	142.9°C/301.96°C
Inlet and outlet temperatures of low-pressure side of recuperator	346.5°C/103.7°C	346.5°C/152.9°C
Minimum temperature difference of recuperator	10.1°C	10.0°C
Turbine produced power	49.8 MW	60.4 MW
Compressor consumed power	13.9 MW	27.8 MW

are kept constant. The effects of compressor parameters on RBC cycle efficiency shown in Figure 12 are similar to what are shown in Figure 8 for SBC. The compressor working close to the critical point or pseudocritical point can achieve the peak cycle efficiency at each CIP value. For CIP ranging from 7.4 to 8.0 MPa, the highest cycle thermal efficiency for RBC is 39.80% when the CIP equals to 7.4 MPa and CIT is about 32°C. At different CIP pressure level, 1°C away from the critical or pseudopoint, brings around 0.3% cycle efficiency reduction. For the conditions whose CIT temperature is away from the critical point, 0.1 MPa CIP increase will result in around 0.2% efficiency increase. This phenomenon is on the contrary to what is found in Figure 8 for SBC. For RBC, the recompression compressor consumed power is more than the power consumed by main compressor because its inlet working condition is far from the critical area. Increasing CIP is helpful to decrease the compressor pressure ratio, which will help decrease the power consumed by recompression compressor and further increase the overall cycle efficiency. This phenomenon indicates that increasing the CIP is helpful to increase overall cycle efficiency for dry-cooled RBC.

4.2.2. Effects of TIP. In order to investigate the effects of TIP on the overall cycle efficiency, other parameters for RBC in Table 4 are kept constant during this sensitivity analysis. Figure 13 shows the variation of cycle efficiency and turbomachinery work with different TIPs. It is easy to see that the cycle efficiency variation with TIP for RBC is different from what is shown in Figure 9 for SBC. For RBC, the cycle efficiency increases with the TIP increase firstly, then reaches the efficiency peak at around TIP of 23 MPa, and after that starts to decrease although the TIP keep increasing. When TIP is lower than 23 MPa, 1 MPa increase in TIP will bring around 1% cycle efficiency increase. When TIP is higher than 23 MPa, 1 MPa increase in TIP will result in 0.2% cycle efficiency decrease. The difference between SBC and RBC is

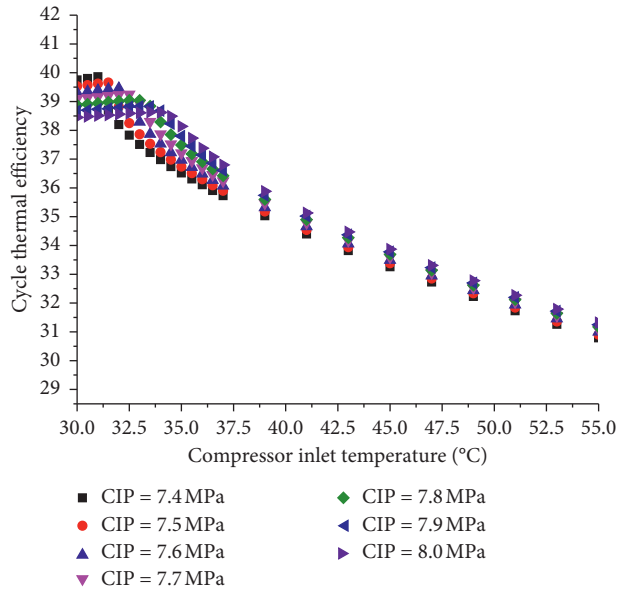

Figure 12: Effects of recuperator UA on the cycle thermal efficiency for RBC.

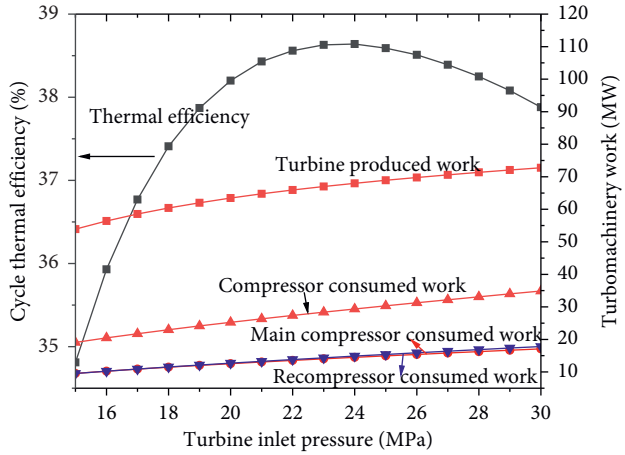

Figure 13: Effects of TIP on the cycle thermal efficiency for RBC.

mainly caused by the introduction of the recompression compressor to the RBC system. The coolant flowing through the recompression compressor works far away from the critical point, which means that the recompression compressor needs more power than the main compressor to compress the same amount of coolant. Increasing TIP not only makes the turbine to produce more power but also consumes more work to drive the compressor. The combined effect of turbine and compressor makes the cycle efficiency decrease with TIP after a certain point.

4.2.3. Effects of Heat Exchanger. A single recuperator has the problem of pinch point, which constraints the cycle efficiency improvement. The cold CO_2 of the low-temperature recuperator has higher specific heat capacity than the hot CO_2 of the low-temperature recuperator. A bypass loop is needed to reduce the cold CO_2 flow rate and balance the capacitance rates of hot and cold CO_2 flow. This is helpful to increase the effectiveness of the low-temperature recuperator. The CO_2 bypassed from the main compressor will be compressed by another compressor and meet with the coolant flowing out of the low-temperature recuperator at a point between the low- and high-temperature recuperators. The system diagram can be found in Figure 3(b).

In the design for the recompression Brayton cycle, there are four factors we need to take into consideration, which are the total recuperator UA, the UA distribution between HTR and LTR, the fraction of coolant flowing through the recompressor, and the working conditions of two recuperators whose min_dt should be less than 10°C. In our calculation, for each total recuperator UA value, the fraction of coolant flowing through the recompressor and the UA distribution between HTR and LTR varies. Under the condition of certain total recuperator UA and certain recompression compressor flow fraction, the UA

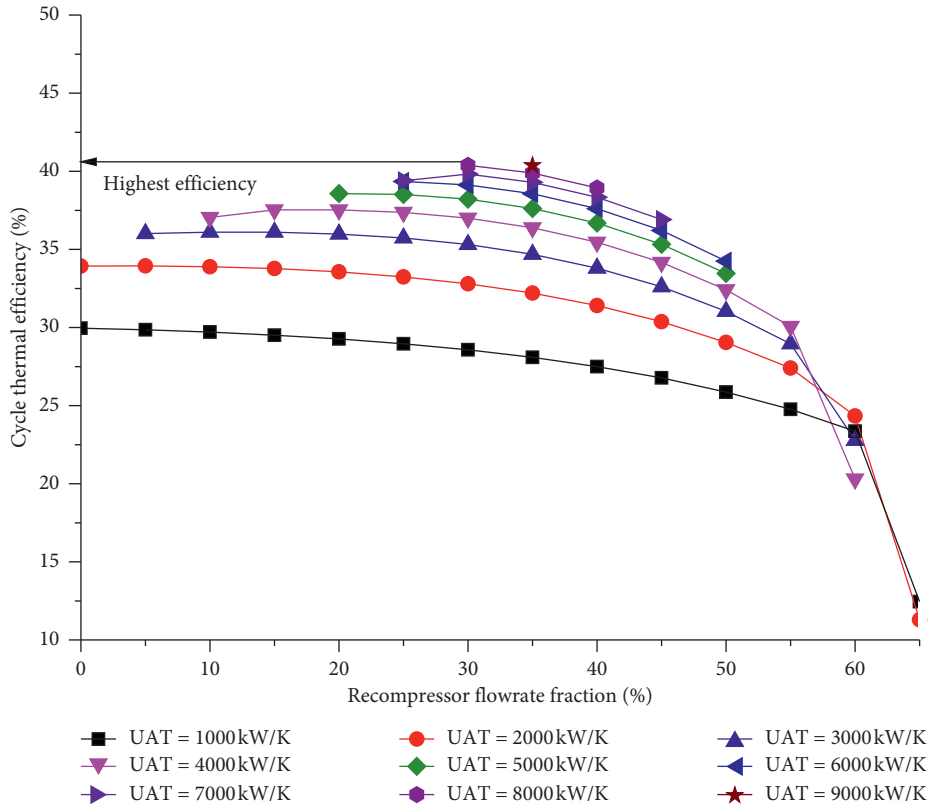

Figure 14: Effects of recuperator UA and recompressor flow rate fraction on the cycle thermal efficiency for water-cooled RBC.

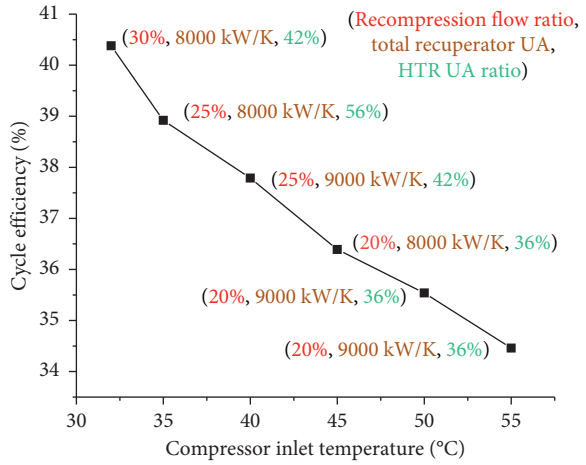

Figure 15: Effects of compressor inlet temperature on the cycle thermal efficiency for dry-cooled RBC.

distribution between HTR and LTR is automatically optimized to achieve the highest cycle efficiency and satisfy the minimum temperature difference for recuperators at the same time. Thus, the cycle thermal efficiency performance at different total recuperator UAs and different recompression compressor flow fractions is obtained, which is shown in Figure 14.

From Figure 14, we can first find that, when total recuperator UA is less than 2000 kW/K, the simple Brayton cycle has a higher cycle thermal efficiency than that of the recompression Brayton cycle. This is mainly because the power consumed by the recompression compressor is higher than the power recovered by the recuperators. When total recuperator UA is higher, RBC starts to show its advantage over SBC. The optimal recompressor flow rate fraction varies at different total recuperator UAs. For the case of total UA equaling to 3000 kW/K, the optimal recompressor flow rate fraction is about 15%, while for case of total UA equaling to 6000 kW/K, it is around 25%. Larger UA value will result in recuperator minimum temperature to be less than 10°C, which is excluded from Figure 14. That is the reason why

Table 6: Optimal design for the water-cooled recompression Brayton cycle.

Cooling type	Water cooled	Dry cooled
Produced net power	40.38 MW	34.36 MW
Cycle thermal efficiency	40.38%	34.36%
Turbine mass flow rate	563.92 kg/s	616.22 kg/s
Recompression flow ratio	30%	20%
TIP/TIT	20 MPa/460°C	20 MPa/460°C
CIP/CIT	7.4 MPa/32°C	7.4 MPa/55°C
HTR UA	3360 kW/K	3240 kW/K
LTR UA	4640 kW/K	5760 kW/K
Inlet and outlet temperatures of high-pressure side of HTR	206.3°C/315.5°C	263.0°C/327.7°C
Inlet and outlet temperature of low-pressure side of HTR	346.5°C/222.1°C	346.5°C/275.0°C
HTR min_dt	15.7°C	12.0°C
Inlet and outlet temperatures of high-pressure side of LTR	94.0°C/207.0°C	142.9°C/262.8°C
Inlet and outlet temperatures of low-pressure side of LTR	222.1°C/104.1°C	275.0°C/154.8°C
LTR min_dt	10.1°C	11.9°C
Turbine produced power	66.11 MW	72.24 MW
Compressor consumed power	42.19 MW	26.6 MW
Recompression compressor consumed power	18.68 MW	11.28 MW

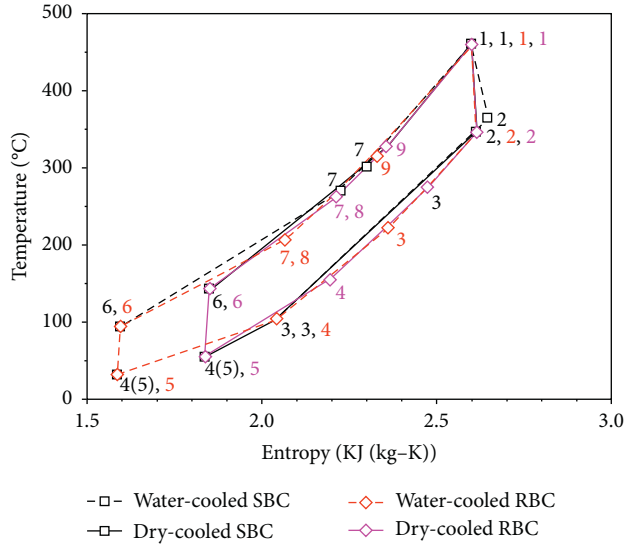

Figure 16: Temperature-entropy comparison among water-cooled and dry-cooled SBC and RBC.

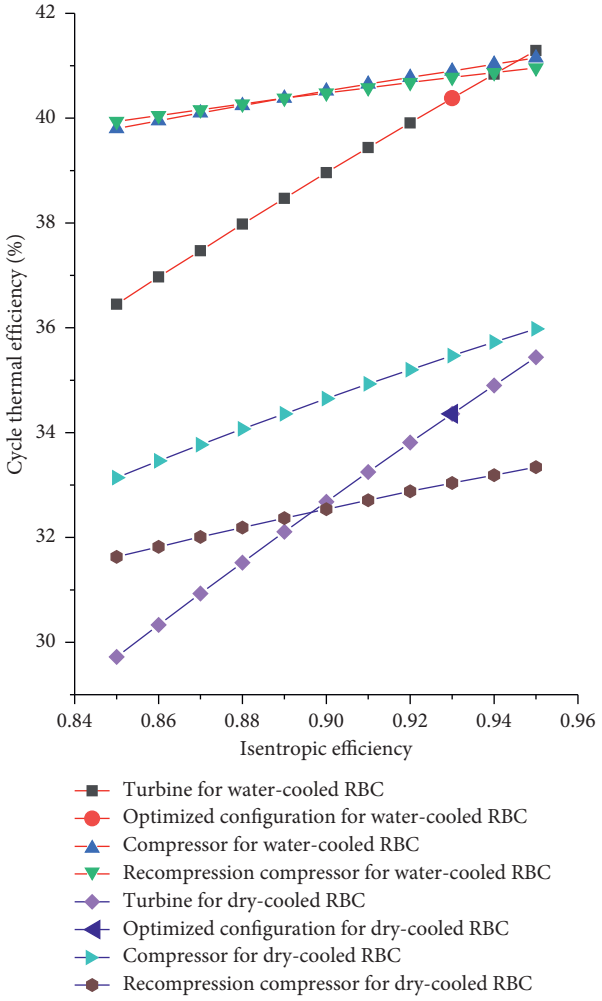

Figure 17: Cycle efficiency variation with turbomachinery for water-cooled and dry-cooled recompression Brayton cycles.

cases whose total UA is larger has less validated points in Figure 14. The cases whose total recuperator UA is higher than 9000 kW/K will make the minimum temperature difference of HTR or LTR less than 10°C and these cases are ignored here.

For the dry-cooled Brayton cycle, the higher compressor inlet temperature results in cycle thermal efficiency decrease. Figure 15 shows the cycle thermal efficiency performance at different compressor inlet temperatures. For each case applying different compressor inlet temperatures, the total recuperator UA, UA distribution between LTR and HTR, and the recompression flow ratio are optimized to get the highest cycle efficiency. From Figure 15, it can be found out that the overall cycle efficiency decreases almost linearly with compressor inlet temperature decrease. Every 5°C increase in CIT will result in around 1.2% cycle efficiency decrease for RBC.

The detailed cycle configuration of optimized RBC for water-cooled (CIT assumed to be 32°C) and dry-cooled conditions (CIT assumed to be 55°C) is listed in Table 6. The entropy and temperature comparison of water-cooled and dry-cooled SBC and RBC are shown in Figure 16.

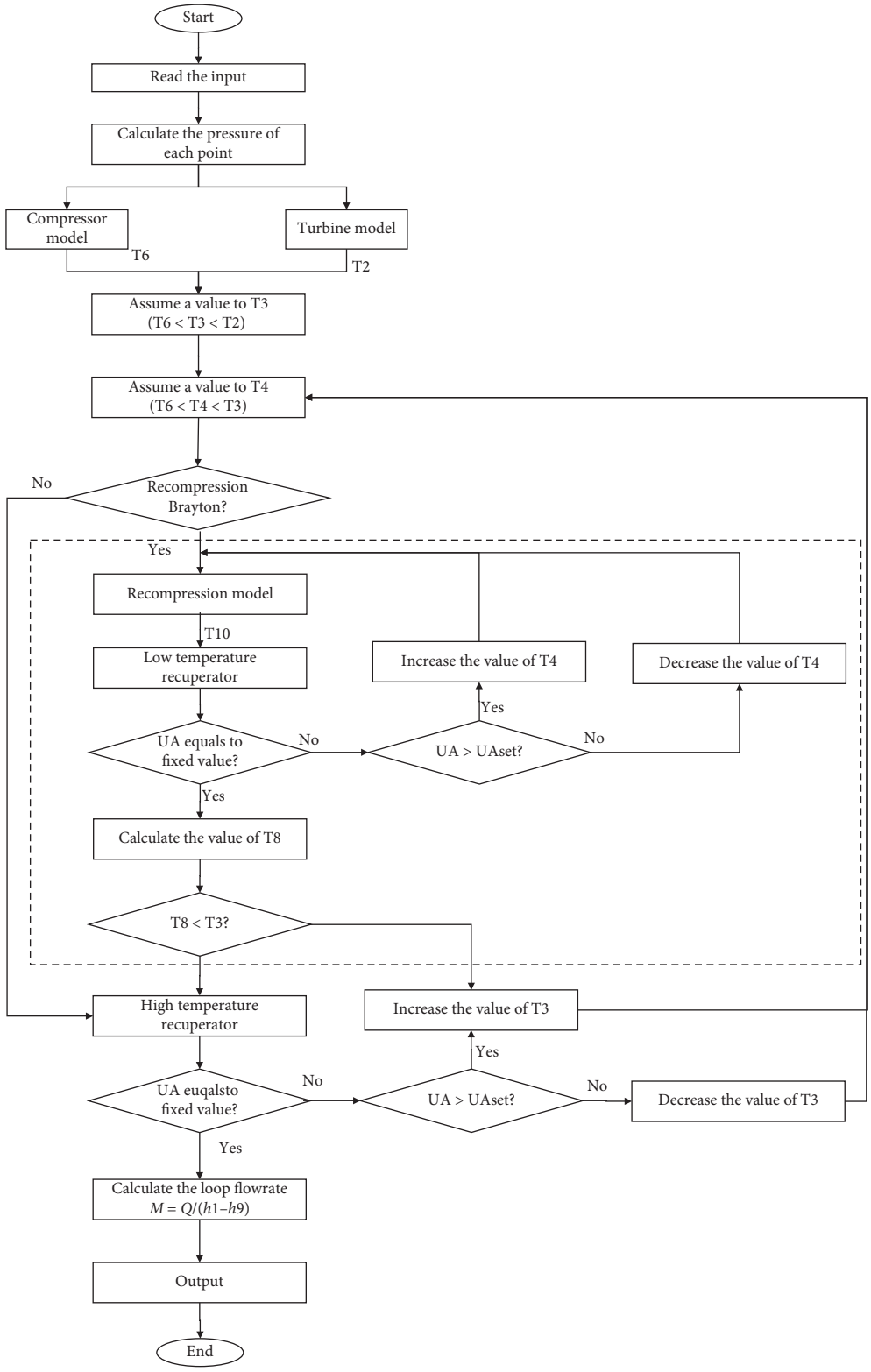

Figure 18: Calculation flowchart of SASCOB.

4.2.4. Turbomachinery Efficiency Effects. Turbomachinery efficiency varies in different literatures. The increase of turbomachinery efficiency helps improve the cycle efficiency. It is obvious from Figure 17 that increasing the turbine efficiency is more efficient in improving the cycle efficiency. Every 1% increase of turbine efficiency will result in 0.5% increase in cycle efficiency for water-cooled RBC and 0.6% increase for dry-cooled RBC. Every 1% increase of the compressor efficiency brings around 0.15% increase in the cycle efficiency for water-cooled RBC and 0.3% increase for

dry-cooled RBC. The recompression compressor efficiency has less impact on cycle efficiency compared with that of the turbine. Every 1% increase of the recompressor brings about 0.1% increase for the recompression Brayton cycle and 0.2% increase for dry-cooled RBC. Conclusion can be made that improving the turbine efficiency is the most effective way to improve the Brayton cycle efficiency.

5. Conclusion

The Brayton cycle design is carried out in this paper for a lead fast reactor concept which owns a core outlet temperature of 480°C. A steady state thermal analysis solver named SASCOB is developed for the S-CO_2 Brayton cycle-cooled reactor. The solver includes necessary modules like heat exchanger, turbomachinery, and CO_2 property package. The solver is capable to obtain the parameters like pressure, temperature, enthalpy, and density along the cycle for simple and recompression Brayton cycles. The accuracy of SASCOB is validated through comparison with the MIT design. With the aid of SASCOB, a feasible simple and recompression Brayton cycle design for the lead fast reactor concept has been achieved under water-cooled and dry air-cooled condition through sensitivity analysis. For SBC, the optimal cycle efficiency can be 35.9% under water-cooled condition (CIT equals to 32°C) and 32.6% under dry air-cooled condition (CIT equals to 55°C) with a turbine inlet temperature of 460°C. For RBC, the optimal cycle efficiency can be 40.48% under water-cooled condition (CIT equals to 32°C) and 34.36% under dry air-cooled condition (CIT equals to 55°C), a turbine inlet temperature of 460°C. The following detailed conclusions can be made:

(1) Here are some discussions about the compressor parameter effect on the overall cycle efficiency. For both SBC and RBC, coolant at the compressor inlet working close to critical or pseudocritical point achieves the highest cycle efficiency. When the compressor inlet temperature is over 35°C, increasing the compressor inlet pressure will result in cycle efficiency decrease for SBC while it will bring cycle efficiency increase for RBC. In the dry air cooling condition, increase the minimum cycle pressure is helpful for RBC because it can help reduce the power consumed by recompression compressor and is harmful for SBC because it can increase the power consumed by the main compressor. When dry air cooling is considered, the CIT is assumed as 55°C, the recuperator UA is set constant, the cycle efficiency of SBC is 4.7% lower than that of SBC cooled by water, while the cycle efficiency of RBC is 9% lower than that of RBC cooled by water.

(2) The effects of TIP on cycle efficiency of SBC and RBC are different. For SBC, higher TIP helps increase the cycle thermal efficiency. However, it is also interesting to see that the efficiency increase rate decreases when turbine inlet pressure is over 20 MPa. For RBC, cycle efficiency increases first and then decreases after reaching a peak value with the increasing turbine inlet pressure. For RBC, increasing TIP not only makes the turbine produce more power but also consumes more work to drive the compressor. The combined effect of turbine and compressor makes the cycle efficiency decrease with TIP after a certain point.

(3) For water-cooled Brayton cycle design (CIT equals to 32°C), when the total recuperator UA is less than 2000 kW/K, SBC has a higher cycle thermal efficiency than RBC. When total recuperator UA is higher, RBC starts to show its advantage over SBC. The optimal recompressor flow rate fraction varies at different total recuperator UAs.

(4) For dry-cooled Brayton cycle design, the optimal cycle efficiency decreases with the CIT increasing from 35°C to 55°C. Every 5°C increase in CIT will result in around 1.2% cycle efficiency decrease for RBC. Increasing the compressor inlet pressure is helpful to increase the overall cycle efficiency for RBC. Every 5°C increase in CIT will result in around 0.7% cycle efficiency decrease for SBC. Compressor inlet pressure moving close to critical pressure is helpful to increase the overall cycle efficiency for SBC.

(5) The increase of turbomachinery help improves the cycle efficiency. For turbomachinery, improving the turbine efficiency is the most effective way to improve the Brayton cycle efficiency. Every 1% increase of turbine efficiency will result in 0.5% increase in cycle efficiency for water-cooled RBC and 0.6% increase for dry-cooled RBC.

The above optimized configuration for SBC and RBC under water-cooled and dry air-cooled conditions will provide promising choices of the power conversion system for the lead fast reactor power. Further system analysis for the lead fast reactor coupled with the S-CO_2 Brayton cycle will be carried out to study the system transient behavior, safety behavior, and control strategy.

Nomenclature

C:	Capacitance rate/ kW/K
W:	Work consumed by turbomachinery, MW
UA:	Heat exchanger conductance, kW/K
Q_{heat}:	Heat source, MW
φ:	Mass flow rate fraction of the recompression compressor
$\dot{m}$:	Mass flow rate, kg·s^{-1}
h:	Enthalpy, J·kg^{-1}
N:	Total number of subheat exchangers
NTU:	Dimensionless number of transfer units (NTUs) for a subheat exchanger
p:	Pressure, MPa
r:	Pressure ratio
s:	Specific entropy, J·(kg·K)$^{-1}$
$c1$:	Compressor inlet
$c2$:	Compressor outlet
$c2s$:	Ideal compressor outlet condition

i: The *i*th number of subheat exchanger
min: Minimum
mc: Main compressor
rc: Recompression compressor
tur: turbine
recom: Recompression compressor
Greek letters:
η: Turbomachinery efficiency
ε: Heat exchanger effectiveness
Acronym:
CIT: Compressor inlet temperature
CIP: Compressor inlet pressure
HX: Heat exchanger
HP: Recuperator's high-pressure side
LFR: Lead fast reactor
LP: Recuperator's low-pressure side
min_dt: Minimum temperature difference
RBC: Recompression Brayton cycle
S-CO_2: Supercritical carbon dioxide
SBC: Simple Brayton cycle
SMR: Small modular reactor
TIT: Turbine inlet temperature
TIP: Turbine inlet pressure.

Appendix

A. Derivation of Recuperator Conductance

In order to reduce the calculation error, the heat exchanger is divided into N parts through the channel. The pressure drop inside the heat exchanger is assumed to be linearly distributed. The cold-side inlet pressure and hot-side outlet pressure of the subheat exchanger can be expressed as follows:

$$\begin{aligned} p_{c,\mathrm{out},i} &= p_{c,\mathrm{in},i} - \frac{i * \Delta p_c}{N}, \\ p_{h,\mathrm{out},i} &= p_{h,\mathrm{in},i} - \frac{i * \Delta p_h}{N}, \end{aligned} \tag{A.1}$$

where $p_{c,in,i}$ denotes the cold-side inlet pressure of the ith subheat exchanger, kPa, $p_{c,\mathrm{out},i}$ denotes the cold-side out pressure, kPa, N denotes the subheat exchanger number, $p_{h,\mathrm{in},i}$ denotes the hot-side inlet pressure of the ith subheat exchanger, kPa, $p_{h,\mathrm{out},i}$, denotes the hot-side outlet pressure of the ith subheat exchanger, kPa, and Δp_h and Δp_c denote the pressure drop through the heat exchanger at hot and cold sides, which will be defined by the user.

With the energy conservation equation, we can get the enthalpy at cold and hot sides of the heat exchanger:

$$\begin{aligned} h_{c,\mathrm{out}} &= h_{c,\mathrm{in}} + \frac{Q}{m_c}, \\ h_{h,\mathrm{out}} &= h_{h,\mathrm{in}} - \frac{Q}{m_h}. \end{aligned} \tag{A.2}$$

The enthalpy inside the heat exchanger is assumed to vary linearly along with the heated or cooled length. Thus, the cold-side inlet and hot-side out enthalpy of each subheat exchanger will be calculated:

$$\begin{aligned} h_{c,\mathrm{in},i} &= h_{c,\mathrm{out},i} + \frac{i * \left(h_{c,\mathrm{in}} - h_{c,\mathrm{out}}\right)}{N}, \\ h_{h,\mathrm{out},i} &= h_{h,\mathrm{in},i} - \frac{i * \left(h_{h,\mathrm{in}} - h_{h,\mathrm{out}}\right)}{N}. \end{aligned} \tag{A.3}$$

The inlet and outlet temperature of each subheat exchanger can be calculated with pressure and enthalpy.

The heat capacity at hot side and cold side of the subheat exchanger can be determined:

$$\begin{aligned} C_{h,i} &= m_h * \frac{h_{h,\mathrm{in},i} - h_{h,\mathrm{out},i}}{T_{h,\mathrm{in},i} - T_{h,\mathrm{out},i}}, \\ C_{c,i} &= m_c * \frac{h_{c,\mathrm{in},i} - h_{c,\mathrm{out},i}}{T_{c,\mathrm{in},i} - T_{c,\mathrm{out},i}}, \\ C_{\min} &= \min\left(C_{h,i}, C_{c,i}\right), \\ C_{\max} &= \max\left(C_{h,i}, C_{c,i}\right), \\ C_R &= \frac{C_{\min}}{C_{\max}}. \end{aligned} \tag{A.4}$$

The effectiveness of the heat exchanger can be calculated with the following equation:

$$\varepsilon_i = \frac{Q}{N * C_{\min,i} * \left(T_{h,\mathrm{in},i} - T_{c,\mathrm{in},i}\right)}. \tag{A.5}$$

And, the UA value of the total heat exchanger can be obtained:

$$\mathrm{UA} = \sum_{i=1}^{N} \left(\mathrm{NTU}_i * C_{\min,i}\right). \tag{A.6}$$

where

$$\mathrm{NTU}_i = \begin{cases} \lg\left(1 - \varepsilon_i C_{R,i} / 1 - \varepsilon_i\right), & C_R \neq 1, \\ \dfrac{\varepsilon_i}{1 - \varepsilon_i}, & C_R = 1. \end{cases} \tag{A.7}$$

B. Calculation Flowchart of SASCOB

Calculation flowchart of SASCOB is given in Figure 18.

Data Availability

The data used to support the findings of this study are available from the corresponding author upon request.

Conflicts of Interest

The authors declare that they have no conflicts of interest.

Acknowledgments

The authors would like to express their special thanks for the financial support from the National Natural Science Foundation of China (Grant Nos.: 11605132 and U1867218) and financial support from the Nuclear Power Institute of China.

References

[1] Y. Ahn, S. J. Bae, M. Kim et al., "Review of supercritical CO_2 power cycle technology and current status of research and development," *Nuclear Engineering and Technology*, vol. 47, no. 6, pp. 647–661, 2015.

[2] M. M. Mohammadi, F. Faghihi, A. Pirouzmand, and A. Rabiee, "Study on the recently proposed direct S-CO_2 and helium-cooled GCFR: size of vessel, power conversion, and reactivity coefficients," *Progress in Nuclear Energy*, vol. 81, pp. 113–122, 2015.

[3] K. Wang and Y.-L. He, "Thermodynamic analysis and optimization of a molten salt solar power tower integrated with a recompression supercritical CO_2 Brayton cycle based on integrated modeling," *Energy Conversion and Management*, vol. 135, pp. 336–350, 2017.

[4] M. T. Luu, D. Milani, R. McNaughton, and A. Abbas, "Dynamic modelling and start-up operation of a solar-assisted recompression supercritical CO_2 Brayton power cycle," *Applied Energy*, vol. 199, pp. 247–263, 2017.

[5] M. A. Pope, J. I. Lee, P. Hejzlar, and M. J. Driscoll, "Thermal hydraulic challenges of gas cooled fast reactors with passive safety features," *Nuclear Engineering and Design*, vol. 239, no. 5, pp. 840–854, 2009.

[6] E. J. Parma, S. A. Wright, M. E. Vernon et al., "Supercritical CO_2 direct cycle Gas Fast Reactor (SC-GFR) concept," *Technical Report*, Sandia National Laboratories, Albuquerque, NM, United States, 2011.

[7] H. Yu, D. Hartanto, B. S. Oh, J. I. Lee, and Y. Kim, "Neutronics and transient analyses of a supercritical CO_2-cooled micro modular reactor (MMR)," *Energy Procedia*, vol. 131, pp. 21–28, 2017.

[8] B. S. Oh, Y. H. Ahn, H. Yu et al., "Safety evaluation of supercritical CO_2 cooled micro modular reactor," *Annals of Nuclear Energy*, vol. 110, pp. 1202–1216, 2017.

[9] Y. Ahn and J. I. Lee, "Study of various Brayton cycle designs for small modular sodium-cooled fast reactor," *Nuclear Engineering and Design*, vol. 276, pp. 128–141, 2014.

[10] J.-E. Cha, T.-H. Lee, J.-H. Eoh et al., "Development of a supercritical CO_2 Brayton energy conversion system coupled with a sodium cooled fast reactor," *Nuclear Engineering and Technology*, vol. 41, no. 8, pp. 1025–1044, 2009.

[11] A. Moisseytsev and J. J. Sienicki, "Transient accident analysis of a supercritical carbon dioxide Brayton cycle energy converter coupled to an autonomous lead-cooled fast reactor," *Nuclear Engineering and Design*, vol. 238, no. 8, pp. 2094–2105, 2008.

[12] P. Wu, C. Gao, and J. Shan, "Development and verification of a transient analysis tool for reactor system using supercritical CO_2 brayton cycle as power conversion system," *Science and Technology of Nuclear Installations*, vol. 2018, Article ID 6801736, 14 pages, 2018.

[13] H. Chen, Z. Chen, C. Chen et al., "Conceptual design of a small modular natural circulation lead cooled fast reactor SNCLFR-100," *International Journal of Hydrogen Energy*, vol. 41, no. 17, pp. 7158–7168, 2016.

[14] J. H. Park, J. Yoon, J. Eoh, H. Kim, and M. H. Kim, "Optimization and sensitivity analysis of the nitrogen Brayton cycle as a power conversion system for a sodium-cooled fast reactor," *Nuclear Engineering and Design*, vol. 340, pp. 325–334, 2018.

[15] V. Dostal, M. J. Driscoll, and P. Hejzlar, *A Supercritical Carbon Dioxide Cycle for Next Generation Nuclear Reactors*, Massachusetts Institute of Technology, Department of Nuclear Engineering, Cambridge, MA, USA, 2004.

[16] X. Zhao, J. Lu, Y. Yuan et al., "Analysis of supercritical carbon dioxide brayton cycle and candidate materials of key hot components for power plants," *Proceedings of the CSEE*, vol. 36, no. 1, pp. 154–162, 2016, in Chinese.

[17] H. S. Pham, N. Alpy, J. H. Ferrasse et al., "Mapping of the thermodynamic performance of the supercritical CO_2 cycle and optimisation for a small modular reactor and a sodium-cooled fast reactor," *Energy*, vol. 87, pp. 412–424, 2015.

[18] T. Neises and C. Turchi, "A comparison of supercritical carbon dioxide power cycle configurations with an emphasis on CSP applications," *Energy Procedia*, vol. 49, pp. 1187–1196, 2014.

[19] J. J. Dyreby, *Modeling the Supercritical Carbon Dioxide Brayton Cycle with Recompression*, The University of Wisconsin-Madison, Madison, WI, USA, 2014.

[20] M. A. Pope, *Thermal Hydraulic Design of a 2400 MWth Direct Supercritical CO_2-cooled Fast Reactor*, Massachusetts Institute of Technology, Cambridge, MA, USA, 2006.

[21] O. Olumayegun, M. Wang, and G. Kelsall, "Thermodynamic analysis and preliminary design of closed Brayton cycle using nitrogen as working fluid and coupled to small modular sodium-cooled fast reactor (SM-SFR)," *Applied Energy*, vol. 191, pp. 436–453, 2017.

[22] A. Moisseytsev and J. J. Sienicki, *Investigation of Plant Control Strategies for a Supercritical CO_2 Brayton Cycle Coupled to a Sodium-Cooled Fast Reactor Using the ANL Plant Dynamics Code*, in *Proceedings of the 2011 Supercritical CO2 Power Cycle Symposium*, Boulder, CO, USA, 2011.

[23] A. Moisseytsev and J. J. Sienicki, "Transient accident analysis of a supercritical carbon dioxide Brayton cycle energy converter coupled to an autonomous lead-cooled fast reactor," in *Proceedings of the 14th International Conference on Nuclear Engineering*, pp. 623–634, American Society of Mechanical Engineers, New York, NY, USA, 2006.

[24] M. A. Reyes-Belmonte, A. Sebastián, M. Romero, and J. González-Aguilar, "Optimization of a recompression supercritical carbon dioxide cycle for an innovative central receiver solar power plant," *Energy*, vol. 112, pp. 17–27, 2016.

[25] Q. H. Deng, D. Wang, H. Zhao, W. T. Huang, S. Shao, and Z. P. Feng, "Study on performances of supercritical CO_2 recompression Brayton cycles with multi-objective optimization," *Applied Thermal Engineering*, vol. 114, pp. 1335–1342, 2017.

[26] T. M. Conboy, M. D. Carlson, and G. E. Rochau, "Dry-cooled supercritical CO_2 power for advanced nuclear reactors," *Journal of Engineering for Gas Turbines and Power*, vol. 137, no. 1, Article ID 012901, 2014.